

Range-Spread Targets Detection in Unknown Doppler Shift via Semi-Definite Programming

Mai P. T. Nguyen, Ickho Song, *Fellow, IEEE*,

Seungwon Lee , and Seokho Yoon, *Senior Member, IEEE*

Abstract

Based on the technique of generalized likelihood ratio test, we address detection schemes for Doppler-shifted range-spread targets in Gaussian noise. First, a detection scheme is derived by solving the maximization associated with the estimation of unknown Doppler frequency with semi-definite programming. To lower the computational complexity of the detector, we then consider a simplification of the detector by adopting maximization over a relaxed space. Both of the proposed detectors are shown to have constant false alarm rate via numerical or theoretical analysis. The detection performance of the proposed detector based on the semi-definite programming is shown to be almost the same as that of the conventional detector designed for known Doppler frequency.

Index Terms

Doppler frequency, generalized likelihood ratio test, range-spread target, semi-definite programming, reduced space.

M. P. T. Nguyen, I. Song, and S. Lee are with the School of Electrical Engineering, Korean Advanced Institute of Science and Technology, Daejeon 34141, Korea (huongmainguyen12@gmail.com, i.song@ieee.org, kkori21@gmail.com).

S. Yoon is with the College of Information and Communication Engineering, Sungkyunkwan University, Suwon 16419, Korea (syoon@skku.edu).

I. INTRODUCTION

In classifying problems of signal detection, we may employ types of signal and noise as a criterion. The types of signal include known deterministic, unknown deterministic, and random signals, and those of noise encompass Gaussian and non-Gaussian noise [1]. Regarding noise, although a non-Gaussian model better represents experimental data and is used in some cases of practical interest [2], the Gaussian model is employed more commonly due to its validity proved by the central limit theorem and mathematical tractability.

In the meantime, while the known deterministic and random signal models arise in a variety of communication problems, the model of deterministic signals with some unknown parameters is commonly found in problems of radar detection [1]. The unknown parameters in problems of radar detection are considered as deterministic quantities or realizations of random variables of known probability density functions (pdf). When the unknown parameters are considered as realizations of random variables, a detector is derived based normally on Bayesian approach. On the other hand, the generalized likelihood ratio test (GLRT) is employed when the unknown parameters are considered as deterministic quantities, in which case the unknown parameters are replaced by their maximum likelihood estimates (MLE) [1], [3].

Among radar detection problems, the detection of range-spread targets with an array of antennas in noise has been addressed in a number of studies including [4]–[10], where the target return is assumed to be known up to a multiplication factor of the steering vector in the cases of non-Gaussian [4], [8], and [10] and Gaussian noise environment [5]–[7], [9]. Specifically, in [5] assuming the availability of the signal-free data, called secondary data, the estimation of the noise covariance matrix is employed in the detection, while a modified GLRT has been proposed in [6] without assuming the availability of secondary data. In [7], detection problem of range-spread targets has been addressed in the case of combined thermal noise and external interference, in which the covariance matrix of noise has the form of an identity matrix plus an unknown positive semi-definite matrix.

The detection schemes considered in [4]–[10] might suffer from a performance loss when the knowledge about the steering vector is imperfect as in the case of mismatched steering vector. To reduce such a detection loss when only the range of steering vector is available, the detection problem has been addressed in several studies [11], [12] under the range models of a linear subspace or a cone class. In essence, the subspace detectors, performing the detection by computing the energy of the measurement in the signal subspace [13] based on linear subspace models, have been considered in [13]–[20]. In the meantime, detectors based on cone class models have been considered in e.g., [21]–[25]: In most cases of the detectors under the cone class models, the likelihood ratios are obtained from numerical methods, and consequently, it is not easy to explain and investigate the detection nature and performance.

In this paper, we consider the problem of detecting range-spread targets in a more general case in which the range of steering vector is unknown, a special case of which is the case of unknown velocity of the target. Adopting an approach similar to that in [30], where the detection of a point-like target is considered, we first derive a GLRT based detection scheme for range-spread targets using a semi-definite programming. A simplified detection scheme is then obtained, which possesses an explicit form of the likelihood ratio and thus incurs less computational complexity. Both of the proposed detectors are shown to not only have the constant false alarm rates (CFAR) but also provide detection probabilities comparable to that of the conventional detector derived with known Doppler frequency.

The rest of this paper is organized as follows. Section II presents the problem formulation and describes details in the derivation of the proposed detectors. Performance analysis and comparison of the detectors discussed in Section III. Section IV concludes this paper.

II. PROBLEM FORMULATION AND PROPOSED DETECTOR

Consider the problem of detecting the presence of a range-spread target, where the potential target is modelled by an unknown range profile (RP) and experiences a motion of unknown velocity relative to the radar. For the detection, reflection from a sequence of N identical coherent

pulses of duty cycle T_D with pulse repetition interval $T_R \gg T_D$ is sampled. We assume that the reflection of the extended target, in case a potential target appears, is completely contained in the first L range bins, whose data is referred to as the primary data. The remaining data, called the secondary data, occupies the remaining K range bins and is composed only of noise (by "noise" we mean radar clutter plus thermal noise). This scenario includes the special case of $L = 1$ (i.e., target is a point scatterer) solved in [26].

Denote the sample at the j -th range bin for the t -th pulse by z_{tj} for $t = 1, 2, \dots, N$ and $j = 1, 2, \dots, L + K$. Arranging the samples collected at range bin j over N consecutive pulses, we can form the $N \times 1$ column vector $\mathbf{z}_j = [z_{1j}, z_{2j}, \dots, z_{Nj}]^T$, where $\{\cdot\}^T$ denotes the transpose of a matrix. The detection problem can now be stated as a problem of choosing between the null hypothesis

$$H_0 : \mathbf{z}_j = \mathbf{n}_j, j = 1, 2, \dots, L + K, \quad (1)$$

and the alternative hypothesis

$$H_1 : \mathbf{z}_j = \begin{cases} \alpha_j \mathbf{p} + \mathbf{n}_j, & j = 1, 2, \dots, L, \\ \mathbf{n}_j, & j = L + 1, L + 2, \dots, L + K. \end{cases} \quad (2)$$

In (1) and (2), the null hypothesis H_0 and alternative hypothesis H_1 denote the cases of noise-only and signal plus noise observations, respectively; the RP α_j represents the response of scatterers at range bin j and is assumed constant during the observation time; and $\mathbf{p} = [1, \exp(j2\pi f_D T_R), \dots, \exp\{j2\pi f_D (N - 1)T_R\}]^T$ accounts for the Doppler shift with f_D the Doppler frequency. In addition, \mathbf{n}_j is an $N \times 1$ zero-mean complex Gaussian noise vector with the common pdf

$$f(\mathbf{n}_j) = \frac{1}{\pi^N |\mathbf{C}|} \exp(-\mathbf{n}_j^H \mathbf{C}^{-1} \mathbf{n}_j) \quad (3)$$

and $N \times N$ positive definite covariance matrix $E[\mathbf{n}_j \mathbf{n}_j^H] = \mathbf{C}$ for $j = 1, 2, \dots, L + K$, where $|\cdot|$ and $\{\cdot\}^H$ denote the determinant and complex conjugate transpose of a matrix, respectively, and $E[\cdot]$ denotes the expectation.

Assuming that the noise vectors $\{\mathbf{n}_i\}_{i=1}^{L+K}$ are independent (that is, $E[\mathbf{n}_i \mathbf{n}_j^H] = \mathbf{0}_{N \times N}$ for $i \neq j$ with $\mathbf{0}_{a \times b}$ the $a \times b$ all-zero matrix) and identically distributed (i.i.d), the joint probability density function (pdf) of the observed data $\{\mathbf{z}_i\}_{i=1}^{L+K}$ can be expressed as

$$f_0(\mathbf{z}_1, \mathbf{z}_2, \dots, \mathbf{z}_{L+K}) = \frac{1}{(\pi^N |\mathbf{C}|)^{L+K}} \exp \left\{ -\text{tr}(\mathbf{C}^{-1} \mathbf{T}_0) \right\} \quad (4)$$

and

$$f_1(\mathbf{z}_1, \mathbf{z}_2, \dots, \mathbf{z}_{L+K}) = \frac{1}{(\pi^N |\mathbf{C}|)^{L+K}} \exp \left\{ -\text{tr}(\mathbf{C}^{-1} \mathbf{T}_1) \right\} \quad (5)$$

under H_0 and H_1 , respectively, where $\text{tr}(\cdot)$ denotes the trace of a square matrix. In (4) and (5),

$$\mathbf{T}_0 = \mathbf{R}(\mathbf{0}_{L \times 1}) + \mathbf{S} \quad (6)$$

and

$$\mathbf{T}_1 = \mathbf{R}(\boldsymbol{\alpha}) + \mathbf{S}, \quad (7)$$

where $\mathbf{R}(\boldsymbol{\alpha}) = \sum_{j=1}^L (\mathbf{z}_j - \alpha_j \mathbf{p})(\mathbf{z}_j - \alpha_j \mathbf{p})^H = (\mathbf{Z} - \mathbf{p} \boldsymbol{\alpha}^T) (\mathbf{Z} - \mathbf{p} \boldsymbol{\alpha}^T)^H$ represents the data in the primary range bins, the matrix $\mathbf{S} = \mathbf{Z}_S \mathbf{Z}_S^H = \sum_{j=L+1}^{L+K} \mathbf{z}_j \mathbf{z}_j^H$ represents the secondary data, and $\boldsymbol{\alpha} = (\alpha_1, \alpha_2, \dots, \alpha_L)^T$ is the $L \times 1$ vector composed of the RP with $\mathbf{Z} = [\mathbf{z}_1, \mathbf{z}_2, \dots, \mathbf{z}_L]$ and $\mathbf{Z}_S = [\mathbf{z}_{L+1}, \mathbf{z}_{L+2}, \dots, \mathbf{z}_{L+K}] = [\mathbf{n}_{L+1}, \mathbf{n}_{L+2}, \dots, \mathbf{n}_{L+K}]$. We will eventually employ some fluctuation models for $\boldsymbol{\alpha}$ later in simulations to account for the variations of the RP over the L range bins. Clearly $\mathbf{R}(\boldsymbol{\alpha})$, \mathbf{S} , \mathbf{Z} , and \mathbf{Z}_S are of sizes $N \times N$, $N \times N$, $N \times L$, and $N \times K$, respectively. Note that the matrix \mathbf{S} is positive semi-definite Hermitian: In addition, it is non-singular with probability one when $K \gg N$. Thus, the matrix \mathbf{S} can be regarded positive definite Hermitian without loss of generality.

From the Neyman-Pearson criterion, the likelihood ratio test (LRT) for the problem of choosing between H_0 and H_1 can now be expressed as

$$\frac{\max_{\mathbf{p}} \max_{\boldsymbol{\alpha}} \max_{\mathbf{C}} f_1(\mathbf{z}_1, \mathbf{z}_2, \dots, \mathbf{z}_{L+K})}{\max_{\mathbf{C}} f_0(\mathbf{z}_1, \mathbf{z}_2, \dots, \mathbf{z}_{L+K})} \underset{H_0}{\overset{H_1}{\gtrless}} G, \quad (8)$$

where the threshold G is chosen based on the desired false alarm rate. Due to the unavailability of \mathbf{p} , noise covariance matrix \mathbf{C} , RP of the target, we resort to a GLRT scheme to derive the LRT,

replacing nuisance parameters with their MLEs under each hypothesis. As it is well-known, the MLE of the noise covariance matrix \mathbf{C} under H_i is \mathbf{T}_i for $i = 0$ and 1 [26]. Direct substitution of the MLEs of the noise covariance matrix \mathbf{C} into (8) leads to

$$\frac{|\mathbf{T}_0|}{\min_{\mathbf{p}} \min_{\boldsymbol{\alpha}} |\mathbf{T}_1|} \underset{H_0}{\overset{H_1}{\geq}} G_1, \quad (9)$$

where $G_1 = \ln G$. The minimization in the denominator over the RP vector $\boldsymbol{\alpha}$ is then attained for [27]

$$\hat{\boldsymbol{\alpha}} = \kappa(\mathbf{p}) (\mathbf{p}^H \mathbf{S}^{-1} \mathbf{Z})^T, \quad (10)$$

where

$$\kappa(\mathbf{p}) = \frac{1}{\mathbf{p}^H \mathbf{S}^{-1} \mathbf{p}} \quad (11)$$

is a positive number since \mathbf{S}^{-1} is positive definite. Hence, the GLRT (9) can be rewritten as

$$\frac{|\mathbf{R}(\mathbf{0}_{L \times 1}) + \mathbf{S}|}{\min_{\mathbf{p}} |\mathbf{R}(\hat{\boldsymbol{\alpha}}) + \mathbf{S}|} \underset{H_0}{\overset{H_1}{\geq}} G_1. \quad (12)$$

After some manipulations as shown in Appendix A, the GLRT is recast as

$$t^\dagger \underset{H_0}{\overset{H_1}{\geq}} G_2, \quad (13)$$

where

$$t^\dagger = \max_{\mathbf{p}} \kappa(\mathbf{p}) \mathbf{p}^H \mathbf{S}^{-1} \mathbf{Z} \mathbf{X}^{-1} \mathbf{Z}^H \mathbf{S}^{-1} \mathbf{p} \quad (14)$$

and G_2 is a suitable modification of G_1 . In (14),

$$\mathbf{X} = \mathbf{I}_L + \boldsymbol{\Upsilon}, \quad (15)$$

where

$$\boldsymbol{\Upsilon} = \mathbf{Z}^H \mathbf{S}^{-1} \mathbf{Z} \quad (16)$$

and \mathbf{I}_L is the $L \times L$ identity matrix. Clearly, $t^\dagger \geq 0$ since $\mathbf{S}^{-1} \mathbf{Z} \mathbf{X}^{-1} \mathbf{Z}^H \mathbf{S}^{-1}$ is positive semi-definite and $\kappa(\mathbf{p})$ is positive. In passing, let us note that, when \mathbf{p} is known, an LRT similar to (13) is derived in [5].

A. Detector based on Semi-Definite Problem

When \mathbf{p} is unknown, the maximization in (14) can be solved by searching over \mathbf{p} , which unfortunately is not quite feasible in practice. We thus change (14) into an equivalent problem for which efficient algorithms can be employed.

Noting that $\mathbf{p} = [1, \exp(j\theta), \dots, \exp\{j(N-1)\theta\}]^T$, where $\theta = 2\pi f_D T_R \in [0, 2\pi)$ is the Doppler phase, let us first rewrite the maximization in (14) as

$$\begin{aligned} & \text{minimize } t \\ & \text{s.t } f(\theta, t) \geq 0, \end{aligned} \tag{17}$$

where

$$f(\theta, t) = ty_0 - x_0 + 2\Re \left\{ \sum_{k=1}^{N-1} (ty_k - x_k) \exp(jk\theta) \right\}. \tag{18}$$

In (18),

$$x_k = \sum_{n-m=k} (\mathbf{S}^{-1} \mathbf{Z} \mathbf{X}^{-1} \mathbf{Z}^H \mathbf{S}^{-1})_{mn} \tag{19}$$

and

$$y_k = \sum_{n-m=k} (\mathbf{S}^{-1})_{mn} \tag{20}$$

for $k = 0, 1, \dots, N-1$, where $(\cdot)_{mn}$ denotes the elements at the m -th row and n -th column and $\Re\{\cdot\}$ denotes the real part. It is easy to see that $x_0 = \text{tr}(\mathbf{S}^{-1} \mathbf{Z} \mathbf{X}^{-1} \mathbf{Z}^H \mathbf{S}^{-1})$ and $y_0 = \text{tr}(\mathbf{S}^{-1})$ are real since $\mathbf{S}^{-1} \mathbf{Z} \mathbf{X}^{-1} \mathbf{Z}^H \mathbf{S}^{-1}$ and \mathbf{S}^{-1} are Hermitian and that the constraint $f(\theta, t) \geq 0$ is derived from, and therefore equivalent to, $t - \kappa(\mathbf{p}) \mathbf{p}^H \mathbf{S}^{-1} \mathbf{Z} \mathbf{X}^{-1} \mathbf{Z}^H \mathbf{S}^{-1} \mathbf{p} \geq 0$.

Now, observe that if $f(\theta, t) \geq 0$ over $\theta \in [0, 2\pi)$ then $t \geq t^\dagger$ and vice versa. In other words, the set $\{t : t \geq t^\dagger\}$ of t is the same as the set $\{t : f(\theta, t) \geq 0, \theta \in [0, 2\pi)\}$ of t . Hence, the solution to the problem (17) is the minimum among the values of t making $f(\theta, t)$ non-negative over $[0, 2\pi)$: To find the minimum, we apply the following theorem, modified from a theorem in [28].

Theorem 1. *The function $f(\theta, t)$ is non-negative over $[0, 2\pi)$ if and only if there exists a matrix $\mathbf{V} \in \mathbb{H}^{N \times N}$ such that*

$$t\mathbf{y} - \mathbf{x} = \mathbf{W}^H \text{diag}(\mathbf{W}\mathbf{V}\mathbf{W}^H). \quad (21)$$

Here, $\mathbb{H}^{N \times N}$ denotes the set of $N \times N$ non-negative definite Hermitian matrices, $\mathbf{y} = [y_0, y_1, \dots, y_{N-1}]^T$, $\mathbf{x} = [x_0, x_1, \dots, x_{N-1}]^T$, $\text{diag}(\cdot)$ denotes the $N \times 1$ vector formed with the diagonal elements, and

$$\mathbf{W} = [\mathbf{w}_0, \mathbf{w}_1, \dots, \mathbf{w}_{N-1}] \quad (22)$$

is an $N \times N$ matrix, where $\mathbf{w}_i = [1, \omega_{M,i}, \dots, \omega_{M,i}^{N-1}]^T$ with $\omega_{M,i} = \exp\left(-j\frac{2\pi i}{M}\right)$ for a number $M \geq 2N - 1$ and $i = 0, 1, \dots, N - 1$.

Applying Theorem 1, the minimization (17) can finally be recast as

$$\begin{aligned} & \text{minimize } t \\ & \text{s.t. } \quad t\mathbf{y} - \mathbf{x} = \mathbf{W}^H \text{diag}(\mathbf{W}\mathbf{V}\mathbf{W}^H), \\ & \quad \mathbf{V} \in \mathbb{H}^{N \times N}. \end{aligned} \quad (23)$$

Since the minimization problem in (23) is a semi-definite problem (SDP), a type of convex optimization problem [28], it can be solved efficiently by various well-known methods such as the interior-point, first-order, and bundle methods [29].

The resulting detector, which will be called the SDP detector, eventually assumes the likelihood ratio test

$$t_C \underset{H_0}{\overset{H_1}{\geq}} G_2, \quad (24)$$

where t_C is the solution of (23) obtained by, for example, the interior-point method.

Theoretically, the performance of the detector (24) would be the same as that of (13). On the other hand, the performance of (13) will in practice depend on the resolution of the searching grid of θ (or equivalently, the unknown Doppler frequency) while the detector (24) is less dependent on the searching grid: In addition, various efficient algorithms can be employed in solving (24) as mentioned above. In passing, let us mention that the study in [30] also applied the result in

[28] for the detection of point-like targets in correlated Gaussian noise under unknown direction of arrival.

B. Detector based on Maximization in the Reduced Space

The processing time to obtain the likelihood ratio t_C from (23) via a semi-definite program increases with the number of range bins (that is, with the range resolution of the radar), as it will be shown later in the numerical results. Another drawback of the likelihood ratio t_C is that it has no explicit form, not allowing an insight into the performance characteristics of a detector such as the CFAR property.

We now derive a detector that can be obtained when the search over \mathbf{p} is replaced with the search over all $N \times 1$ complex vectors. With this relaxation, we can move a few steps further in simplifying, and explicitly showing, the structure of the detector. Of course, since we do not exploit *a priori* knowledge about \mathbf{p} , the simplification is achieved at the expense of some performance loss, and therefore, the detector will have a lower detection probability than its original version.

Firstly, as \mathbf{S}^{-1} is Hermitian, we have $\mathbf{S}^{-1} = \mathbf{U}_{S^{-1}}^H \mathbf{\Lambda}_{S^{-1}} \mathbf{U}_{S^{-1}}$ from the unitary similarity [31], where $\mathbf{U}_{S^{-1}}$ is an $N \times N$ unitary matrix such that $\mathbf{U}_{S^{-1}}^H = \mathbf{U}_{S^{-1}}^{-1}$ and $\mathbf{\Lambda}_{S^{-1}}$ is the $N \times N$ diagonal matrix composed of the eigenvalues $\{\lambda_i\}_{i=1}^N$ of \mathbf{S}^{-1} . Note that the diagonal elements $\{\lambda_i\}_{i=1}^N$ of $\mathbf{\Lambda}_{S^{-1}}$ are all positive with probability one since \mathbf{S}^{-1} is positive definite with probability one. Defining the $N \times 1$ vector

$$\mathbf{l} = \mathbf{\Lambda}_{S^{-1}}^{1/2} \mathbf{U}_{S^{-1}} \mathbf{p} \quad (25)$$

and $N \times L$ matrix

$$\mathbf{Y} = \mathbf{\Lambda}_{S^{-1}}^{1/2} \mathbf{U}_{S^{-1}} \mathbf{Z}, \quad (26)$$

we have $\mathbf{l}^H \mathbf{l} = \mathbf{p}^H \mathbf{S}^{-1} \mathbf{p} = \frac{1}{\kappa(\mathbf{p})}$ and $\mathbf{l}^H \mathbf{Y} = \mathbf{p}^H \mathbf{S}^{-1} \mathbf{Z}$, where $\mathbf{\Lambda}_{S^{-1}}^{1/2}$ is the $N \times N$ diagonal matrix with diagonal elements $\{\sqrt{\lambda_i}\}_{i=1}^N$. Thus, the right-hand side in (14) can be rewritten as

$$\max_{\mathbf{l}} \frac{\mathbf{l}^H \mathbf{Y} (\mathbf{I}_L + \mathbf{\Upsilon})^{-1} \mathbf{Y}^H \mathbf{l}}{\mathbf{l}^H \mathbf{l}}. \quad (27)$$

Here, it should be noticed that the ratio in (27) without \max_l is the Rayleigh quotient [32] of the Hermitian matrix $\mathbf{Y}(\mathbf{I}_L + \mathbf{\Upsilon})^{-1}\mathbf{Y}^H$ at l : An important implication of this fact is that the maximum of the ratio, or equivalently, the solution to (27) over all $N \times 1$ vectors is the same as the maximum eigenvalue of $\mathbf{Y}(\mathbf{I}_L + \mathbf{\Upsilon})^{-1}\mathbf{Y}^H$.

Now, denoting by $\text{eig}\{\cdot\}$ the set of non-zero eigenvalues, we have

$$\begin{aligned} \text{eig}\{\mathbf{Y}(\mathbf{I}_L + \mathbf{\Upsilon})^{-1}\mathbf{Y}^H\} &= \text{eig}\{(\mathbf{I}_L + \mathbf{\Upsilon})^{-1}\mathbf{Y}^H\mathbf{Y}\} \\ &= \text{eig}\{(\mathbf{I}_L + \mathbf{\Upsilon})^{-1}\mathbf{\Upsilon}\}, \end{aligned} \quad (28)$$

where the first equality is based on the fact that $\text{eig}\{\mathbf{A}\mathbf{B}\} = \text{eig}\{\mathbf{B}\mathbf{A}\}$ for any $m \times n$ matrix \mathbf{A} and $n \times m$ matrix \mathbf{B} [33] and the second equality is from $\mathbf{Y}^H\mathbf{Y} = (\mathbf{\Lambda}_{S^{-1}}^{1/2}\mathbf{U}_{S^{-1}}\mathbf{Z})^H \mathbf{\Lambda}_{S^{-1}}^{1/2}\mathbf{U}_{S^{-1}}\mathbf{Z} = \mathbf{Z}^H\mathbf{U}_{S^{-1}}^H (\mathbf{\Lambda}_{S^{-1}}^{1/2})^H \mathbf{\Lambda}_{S^{-1}}^{1/2}\mathbf{U}_{S^{-1}}\mathbf{Z} = \mathbf{\Upsilon}$. Since $\mathbf{\Upsilon} = \mathbf{Z}^H\mathbf{S}^{-1}\mathbf{Z}$ is Hermitian, we have the decomposition

$$\mathbf{\Upsilon} = \mathbf{U}_{\Upsilon}^H \mathbf{\Lambda}_{\Upsilon} \mathbf{U}_{\Upsilon} \quad (29)$$

where $\mathbf{\Lambda}_{\Upsilon}$ is the $L \times L$ diagonal matrix composed of the eigenvalues $\{d_i\}_{i=1}^L$ of $\mathbf{\Upsilon}$ and \mathbf{U}_{Υ} is an $L \times L$ unitary matrix. Thus, we get

$$\begin{aligned} \text{eig}\{(\mathbf{I}_L + \mathbf{\Upsilon})^{-1}\mathbf{\Upsilon}\} &= \text{eig}\{(\mathbf{I}_L + \mathbf{U}_{\Upsilon}^H \mathbf{\Lambda}_{\Upsilon} \mathbf{U}_{\Upsilon})^{-1} \mathbf{U}_{\Upsilon}^H \mathbf{\Lambda}_{\Upsilon} \mathbf{U}_{\Upsilon}\} \\ &= \text{eig}\{[\mathbf{U}_{\Upsilon}^H (\mathbf{I}_L + \mathbf{\Lambda}_{\Upsilon}) \mathbf{U}_{\Upsilon}]^{-1} \mathbf{U}_{\Upsilon}^H \mathbf{\Lambda}_{\Upsilon} \mathbf{U}_{\Upsilon}\} \\ &= \text{eig}\{\mathbf{U}_{\Upsilon}^H (\mathbf{I}_L + \mathbf{\Lambda}_{\Upsilon})^{-1} \mathbf{\Lambda}_{\Upsilon} \mathbf{U}_{\Upsilon}\} \\ &= \text{eig}\{(\mathbf{I}_L + \mathbf{\Lambda}_{\Upsilon})^{-1} \mathbf{\Lambda}_{\Upsilon}\}, \end{aligned} \quad (30)$$

where we have used $\mathbf{U}_{\Upsilon}^{-1} = \mathbf{U}_{\Upsilon}^H$ in the third equality and the last equality is based on the fact that $\text{eig}\{\mathbf{A}\} = \text{eig}\{\mathbf{B}^{-1}\mathbf{A}\mathbf{B}\}$ when \mathbf{A} and \mathbf{B} are square matrices of the same size and \mathbf{B} is invertible [34].

The matrix $(\mathbf{I}_L + \mathbf{\Lambda}_{\Upsilon})^{-1} \mathbf{\Lambda}_{\Upsilon}$ is diagonal, and therefore, its eigenvalues are the same as its elements $\left\{\frac{d_i}{1+d_i}\right\}_{i=1}^L$ since $\mathbf{\Upsilon}$ is positive semi-definite, where $d_i \geq 0$ for $i = 1, 2, \dots, L$. Noting that $\frac{x}{1+x}$ is an increasing function of $x \geq 0$, it is easy to see that the maximum

eigenvalue of $(\mathbf{I}_L + \mathbf{\Lambda}_\Upsilon)^{-1} \mathbf{\Lambda}_\Upsilon$, that is, the maximum value of (27) is $\frac{d_{\max}}{1 + d_{\max}}$ with $d_{\max} = \max\{d_1, d_2, \dots, d_L\}$.

The resulting detector, which we call the maximization in the relaxed space (MRS) detector, is thus based on the likelihood ratio test

$$\frac{d_{\max}}{1 + d_{\max}} \underset{H_0}{\overset{H_1}{\gtrless}} \tilde{G}_2, \quad (31)$$

where \tilde{G}_2 is the threshold. In Appendix B, it is shown that the MRS detector (31) possesses the CFAR property.

III. NUMERICAL RESULTS

In this section, we assess and compare the performance, the probabilities of detection and false alarm, of the proposed detectors (24) and (31) with that of the conventional detector

$$\frac{\mathbf{p}^H \mathbf{S}^{-1} \mathbf{Z} \mathbf{X}^{-1} \mathbf{Z}^H \mathbf{S}^{-1} \mathbf{p}}{\mathbf{p}^H \mathbf{S}^{-1} \mathbf{p}} \underset{H_0}{\overset{H_1}{\gtrless}} \tilde{G}_3 \quad (32)$$

derived when \mathbf{p} is known, where \tilde{G}_3 is a threshold. The detector represented by (32) will be called the one-step GLRT (OS-GLRT) [5]. In short, (32) is an ideal detector, of which the performance represents the bound of other detectors designed for unknown \mathbf{p} .

A. Parameters

The detection performance of three detectors was assessed with $N = 8$ identical coherent pulses transmitted with the pulse repetition interval $T_R = 40 \mu\text{s}$ and Doppler frequency $f_D = 10$ kHz (which corresponds to a velocity of 150 m/s for a wavelength of $\lambda = 3$ cm). The number L of range cells in the primary data is lower bounded by the ratio of the range extent of a target to the range resolution of the radar and it could be of several hundreds [5]. To alleviate the computational burden, we chose $L = 8, 12, 16$, and 20 with the energy distribution among scatterers as shown in Table I. The size of the secondary data is chosen as $K = 16N = 128$ so that the matrix \mathbf{S} of the secondary data is non-singular. For use in (22), we have chosen $M = 2N - 1 = 15$. Finally, we use the software CVX (<http://cvxr.com/>) to solve the semi-definite problem (23) on a computer equipped with a 3.4 GHz Intel processor.

TABLE I
ENERGY DISTRIBUTION AT DISCRETE SCATTERER LOCATIONS WHEN $L = 8, 12, 16,$ AND 20

$L = 8$	0	$\frac{1}{16}$	0	$\frac{1}{2}$	$\frac{1}{4}$	$\frac{1}{16}$	$\frac{1}{8}$	0											
$L = 12$	0	$\frac{1}{16}$	$\frac{1}{16}$	0	0	0	$\frac{1}{16}$	$\frac{1}{16}$	$\frac{1}{2}$	$\frac{1}{4}$	0	0							
$L = 16$	0	0	$\frac{1}{32}$	$\frac{1}{32}$	0	$\frac{1}{2}$	$\frac{1}{4}$	0	$\frac{1}{32}$	0	$\frac{1}{16}$	$\frac{1}{32}$	0	$\frac{1}{16}$	0				
$L = 20$	0	$\frac{1}{10}$	0	$\frac{1}{10}$	0	$\frac{1}{10}$	0	$\frac{1}{10}$	0	$\frac{1}{10}$	0	$\frac{1}{10}$	0	$\frac{1}{10}$	0	$\frac{1}{10}$	0	$\frac{1}{10}$	$\frac{1}{10}$

B. Simulation Results and Discussion

The performance of the SDP and MRS detectors are assessed for the detection of steady and fluctuating targets embedded in Gaussian noise of various correlation degrees in comparison with the OS-GLRT detector. In addition, the complexities of the three detectors are considered in terms of the average processing time. Since it is not plausible to derive explicit forms of the false alarm and detection probabilities, we resort to Monte Carlo trials, in which we set the false alarm rate at 10^{-4} . Since the MRS and OS-GLRT detectors possess CFAR property as shown in Appendix B and in [5], respectively, the thresholds of the MRS and OS-GLRT detectors are determined once. The threshold of the SDP detector are, on the other hand, determined for each noise covariance.

1) *Threshold of the SDP detector:* We first investigate if the SDP detector also has a CFAR property. Here, correlated noise vectors with covariance matrix

$$\mathbf{C} = \sigma_n^2 \begin{bmatrix} 1 & \rho & \dots & \rho^{N-1} \\ \rho & 1 & \dots & \rho^{N-2} \\ \vdots & \vdots & \ddots & \vdots \\ \rho^{N-1} & \rho^{N-2} & \dots & 1 \end{bmatrix} \quad (33)$$

are employed, where σ_n^2 and ρ denote the average noise power at one range cell and the one-lag correlation coefficient, respectively.

Fig. 1 shows the false alarm rates P_{fa} of the SDP detector as a function of threshold at various values of ρ when $\sigma_n^2 = 1$. It is observed from the figure that the threshold for a specific value

of P_{fa} does not depend on ρ . We believe this observation is a natural consequence since the likelihood ratio of the SDP detector is a close approximation to that of the OS-GLRT detector, which possesses a CFAR property.

2) *Detection performance with steady targets:* We now evaluate the detection performance of proposed detectors when the RP of a potential target remains constant during the observation time. The performances are investigated at velocities $v = -100, 120, 150, \text{ and } 180$ m/s corresponding to Doppler frequencies $f_D = -6.67, 8, 10, \text{ and } 12$ KHz, respectively. In the evaluation, we assume $L = 8$ and $\rho = 0.4$. The detection probabilities P_d are shown in Fig. 2 as a function of the signal-to-noise ratio (SNR) defined as

$$\text{SNR} = \frac{\|\mathbf{p}\|^2 \sum_{i=1}^L |\alpha_i|^2}{LN\sigma_n^2}. \quad (34)$$

It is observed from Fig. 2 that the SDP detector achieves nearly the same performance as the OS-GLRT detector and outperforms the MRS detector. For example, the SDP detector provides a gain of around 1.4 dB over the MRS detector for all the values of f_D . To explain, we recall that information about the form of a target's return $\mathbf{p} = [1, \exp(j2\pi f_D T_R), \dots, \exp\{j2\pi f_D (N-1)T_R\}]^T$ is exploited in the SDP detector; yet to the MRS detector such information is not exploited.

Assume $L = 8$, we next assess detection probabilities in noise with various ρ : 0, 0.4, and 0.9. It is shown from Fig. 3 that with proposed detectors, a higher value of ρ associates to a better detection performance. For example, at $\text{SNR} = -10$ dB, with $\rho = 0.9$ proposed detectors yield $P_d = 1$; yet with $\rho = 0.4$ the SDP detector yields $P_d \approx 0.3$ and the MRS detector yields $P_d \approx 0.1$. When ρ approaches 1, for example, $\rho = 0.999$ (for brevity simulation result are not presented), all detectors achieve $P_d = 1$ at $\text{SNR} = -25$ dB. This observation is intuitively reasonable since a higher value of ρ implies more similarity between noise samples, i.e., more information about noise, which possibly leads to a better detection performance.

3) *Detection performance with fluctuating targets:* Let us next address detection performances of proposed detectors when a potential target's RP fluctuates. Firstly, we describe how we generate a fluctuating RP. We note that target's radar cross section (RCS) representing the total energy

reflected from the target also fluctuates with a fluctuating RP target. In addition, such fluctuating RCS is well described by the Swerling models [36]. Based on [35], we derive the relationship between a target's RCS, denoted by σ , and its RP

$$\sigma \propto \frac{1}{2} \sum_{j=1}^L |\alpha_j|^2. \quad (35)$$

We now assume that, for simplicity, all main scatterers on the target follow a same fluctuating pattern. With this assumption and existing models of fluctuating σ , the generation of a fluctuating RP is straightforward. We employ, in the evaluation, Swerling II and IV models, and we use $L = 8$. Note that Swerling II and IV models are chi squared distributions of 2 and 4 degrees of freedom, respectively. Therefore, a Swerling II variable exhibits larger covariance, i.e. more fluctuation, than a Swerling IV variable at a same expectation. In the sequel, we refer a target with Swerling II or IV RCS as a Swerling II or IV target, respectively. The averaged SNR is defined as

$$\text{SNR}_{av} = \frac{E \left[\|\mathbf{p}\|^2 \sum_{i=1}^L |\alpha_i|^2 \right]}{LN\sigma_n^2} \propto \frac{2\bar{\sigma} \|\mathbf{p}\|^2}{LN\sigma_n^2}, \quad (36)$$

where *av* stands for 'averaged' and $\bar{\sigma}$ the average of a target's RCS.

In Figs. 4 and 5, we show detection probabilities P_d of proposed detectors, in comparison with the OS-GLRT detector, as functions of the averaged SNR. These figures highlight observations identical to those derived from Figs 2 and 3.

The order of performance in terms of target's type are steady, Swerling IV, and Swerling II. Lower probabilities in the detection of a fluctuating target, compared to a steady target, is expected since fluctuation in a target's RP is not considered in the design stage of the three detectors. Similarly, since a Swerling II target's return exhibits more fluctuation than that of a Swerling IV target, detection probability with a Swerling II target is lower than that with a Swerling IV target.

4) *Detection with incorrect information about Doppler frequency:* In Fig. 6, we compare the detection performance of the proposed detectors with that of the OS-GLRT detector when

TABLE II
AVERAGE COMPUTATIONAL TIME (IN SECOND) OF OS-GLRT, MRS, AND SDP DETECTORS

	$L = 8$	$L = 12$	$L = 16$	$L = 20$
OS-GLRT	2.44×10^{-4}	2.85×10^{-4}	3.32×10^{-4}	3.88×10^{-4}
MRS	3.55×10^{-4}	3.63×10^{-4}	4.87×10^{-4}	6.12×10^{-4}
SDP	1.53×10^{-1}	1.59×10^{-1}	2.01×10^{-1}	2.03×10^{-1}

information about Doppler frequency is incorrect. In the evaluation, the pre-assumed Doppler frequency is 10 KHz, yet the actual value is 12 KHz. We use $L = 8$, $\rho = 0.4$, and a steady RP. We observe that the SDP and the MRS detectors outperform the OS-GLRT detector with performance gaps, for example at $\text{SNR} = -10$ dB, of about 6 and 5 dB, respectively. This observation is easily anticipated since the operations of the SDP and the MRS detectors do not require Doppler frequency information; however, the OS-GLRT detector requires an exact information about Doppler frequency.

5) *Complexity of proposed detectors:* Finally, we consider the complexity of proposed detectors in terms of average time consumption (in second). Here, we assess time consumption with different RP's length $L = 8, 12, 16$, and 20. For each detector, computational time is averaged over 1000 repetitions to make results reliable.

It is shown in Table II, as easily anticipated, that the SDP detector assumes much more processing time, which is in an order of 10^{-1} , than the MRS and the OS-GLRT detectors, whose processing time are in the order of 10^{-4} . Besides the computation shared by all detectors, the MRS detector computes the maximum eigenvalue of $\mathbf{Z}^H \mathbf{S}^{-1} \mathbf{Z}$, which exhibits a little more computation than the matrix multiplications $\mathbf{p}^H \mathbf{S}^{-1} \mathbf{Z} \mathbf{X}^{-1} \mathbf{Z}^H \mathbf{S}^{-1} \mathbf{p}$ and $\mathbf{p}^H \mathbf{S}^{-1} \mathbf{p}$ implemented in the OS-GLRT detector. For the SDP detector, to implement the semi-definite programming (23) exhibits even much more computation.

We notice that the SDP detector's computational complexity is unsuitable for a radar scan mode. Yet, though possessing fast implementation, the MRS detector may miss a target due to

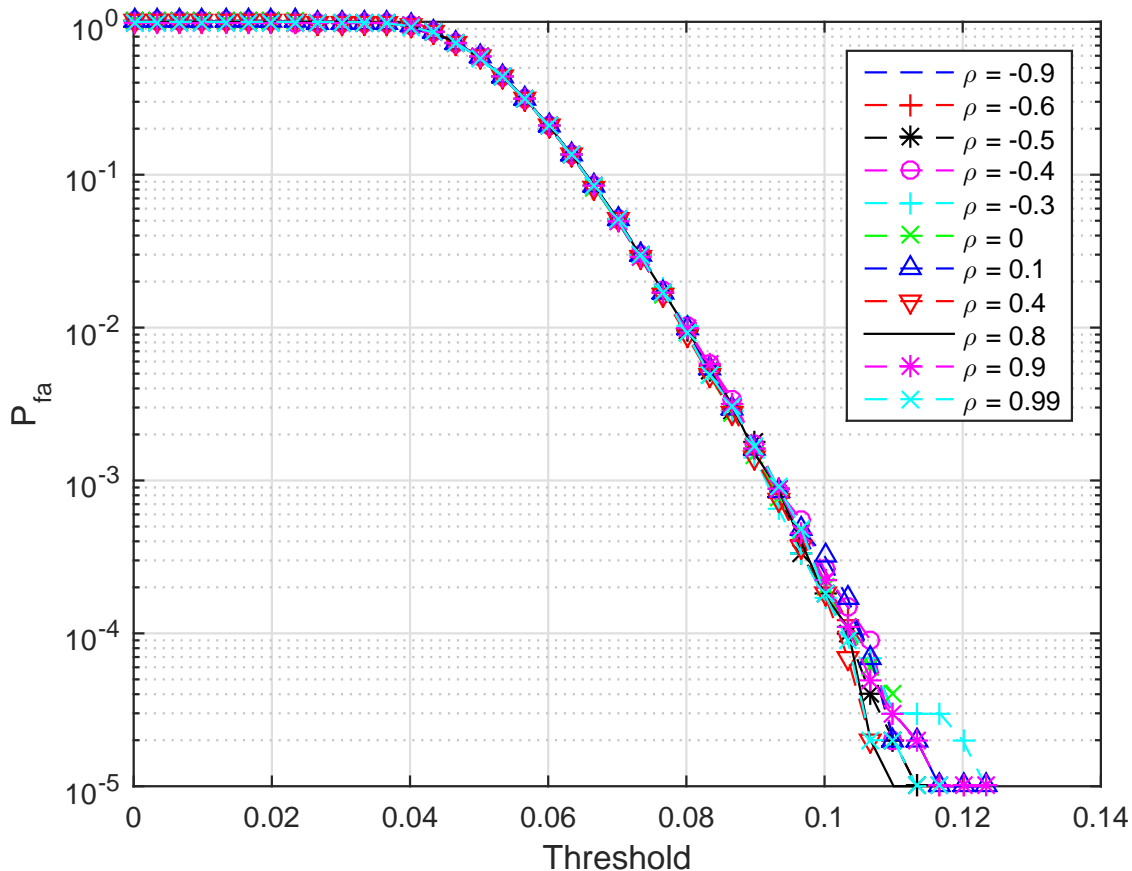


Fig. 1. False alarm probability versus thresholds of the SDP detector.

lower detection performance, for which a measure is to increase transmitted power.

IV. CONCLUSION

We have proposed GLRT-based detectors for a range-spread target of unknown Doppler frequency embedded in Gaussian noise. Regarding the SDP detector, we resort to a semi-definite programming to solve the optimization problem associated to the MLE of unknown Doppler frequency. To reduce the implementation complexity of the SDP detector, we then address a suboptimal detector by solving the above optimization over a relaxed space. Performance of proposed detectors have been assessed, in comparison with the conventional detector derived with known Doppler frequency, in noise of various correlation degrees and with steady and

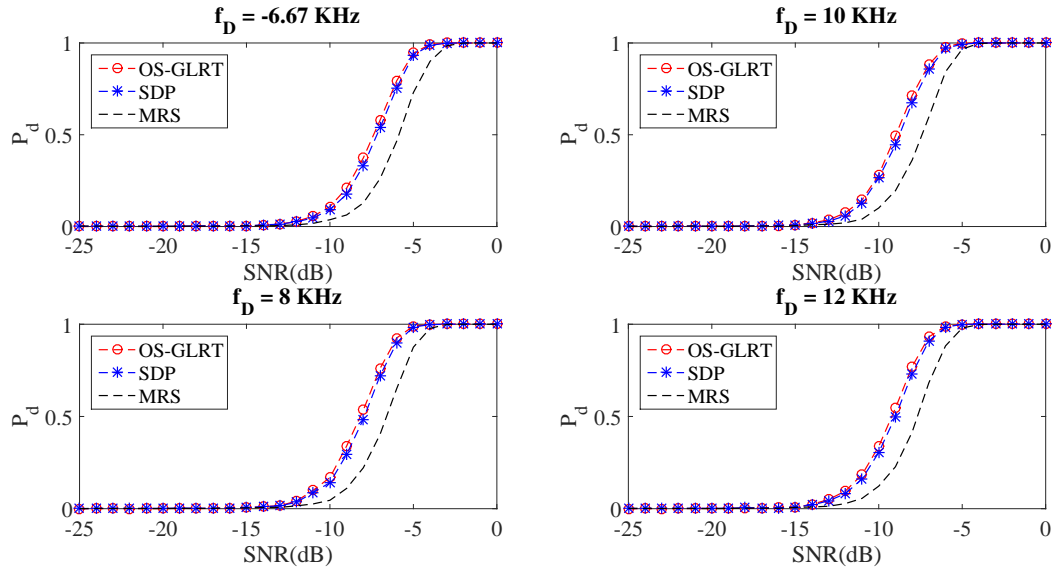


Fig. 2. Detection probability of the SDP and MRS versus OS-GLRT detectors, steady target.

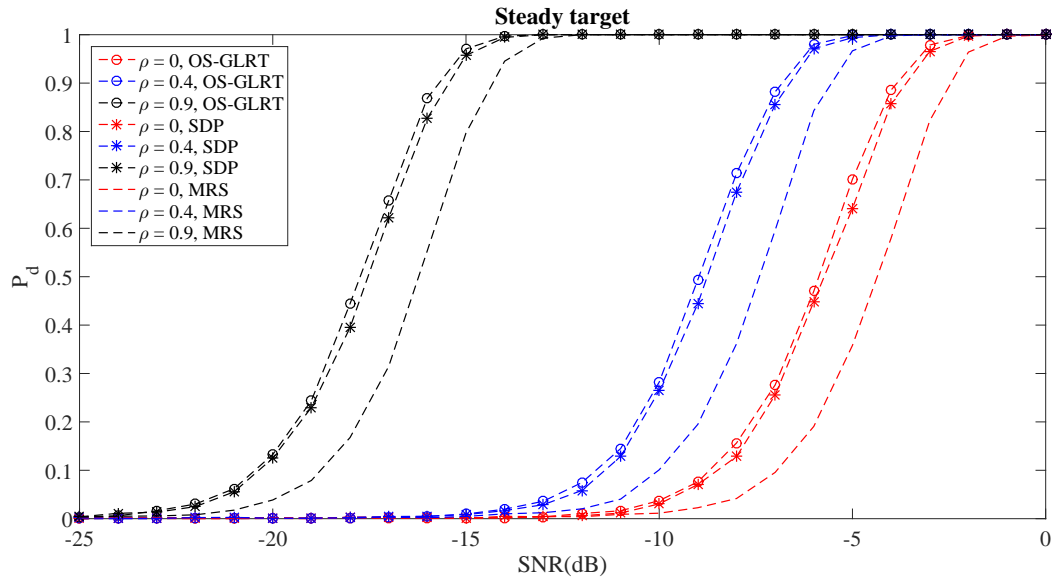


Fig. 3. Detection probability of the SDP and MRS versus OS-GLRT detectors, steady target.

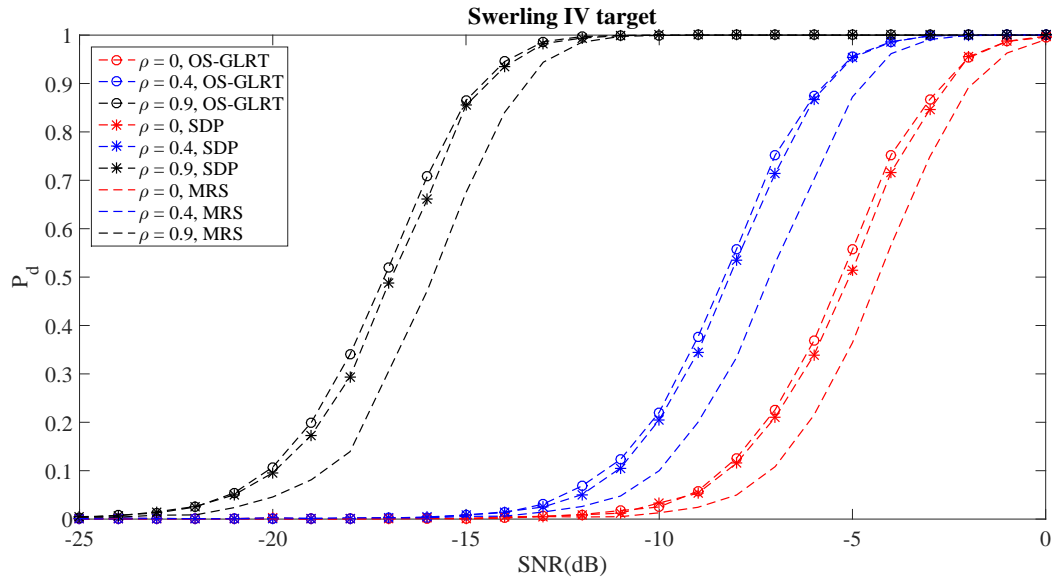


Fig. 4. Detection probability of the SDP and MRS versus OS-GLRT detectors, Swerling IV target.

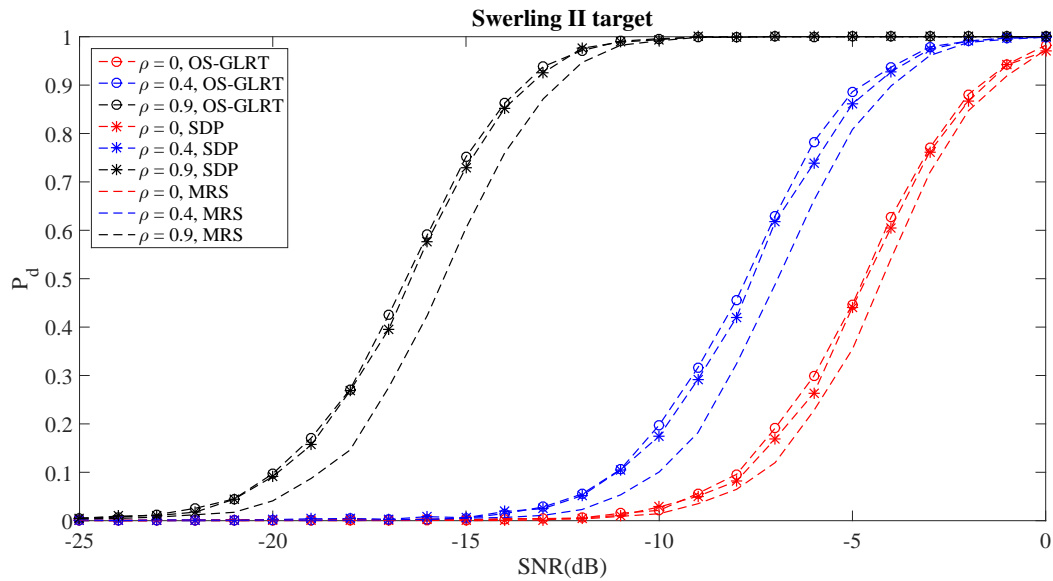


Fig. 5. Detection probability of the SDP and MRS versus OS-GLRT detectors, Swerling II target.

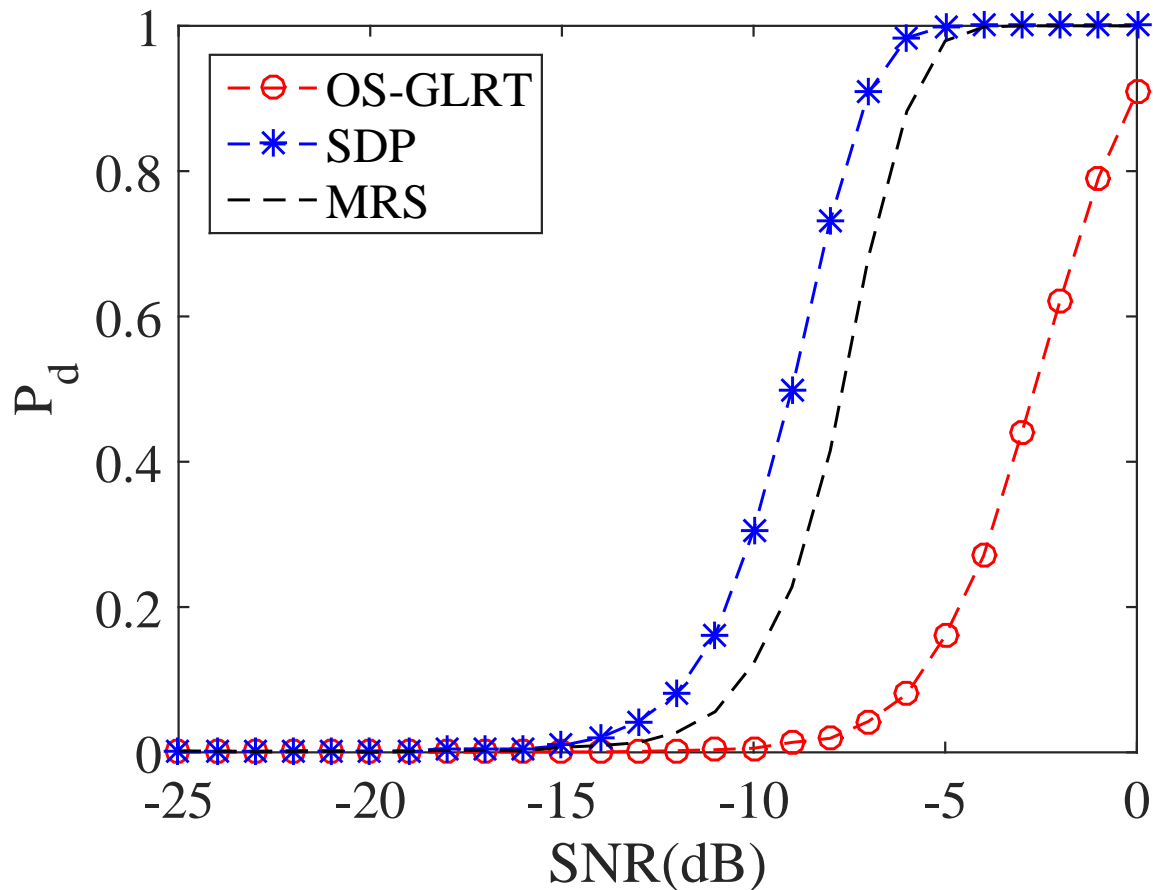


Fig. 6. Detection probability of the SDP and MRS versus OS-GLRT detectors, Steady target when information about target's velocity is not correct.

fluctuating targets. It is observed that the detection gap between the SDP detector and the conventional detector is negligible. In addition, performance of the MRS detector could be considered as a lower bound for GLRT-based detectors when no information about a potential target is available. Both proposed detectors have been proved, theoretically or numerically, to possess CFAR.

The main drawback of this paper is the lack of closed forms for detection and false alarm probabilities of the proposed detectors, which is for a future research. Also, we plan to consider the detection problem under a more generalized noise model, the spherically invariant random

process.

APPENDIX A

PROOF OF THE PROPOSED GLRT (13)

Let us first show the equality

$$(\mathbf{Z} - \mathbf{p}\hat{\boldsymbol{\alpha}}^T)^H \mathbf{S}^{-1} (\mathbf{Z} - \mathbf{p}\hat{\boldsymbol{\alpha}}^T) = \Upsilon - \kappa(\mathbf{p}) \mathbf{u}\mathbf{u}^H, \quad (37)$$

where

$$\mathbf{u} = \mathbf{Z}^H \mathbf{S}^{-1} \mathbf{p}. \quad (38)$$

Firstly, if we expand the left-hand side of (37), we have

$$\begin{aligned} (\mathbf{Z} - \mathbf{p}\hat{\boldsymbol{\alpha}}^T)^H \mathbf{S}^{-1} (\mathbf{Z} - \mathbf{p}\hat{\boldsymbol{\alpha}}^T) &= \Upsilon - \hat{\boldsymbol{\alpha}}^* \mathbf{p}^H \mathbf{S}^{-1} \mathbf{Z} - \mathbf{Z}^H \mathbf{S}^{-1} \mathbf{p} \hat{\boldsymbol{\alpha}}^T \\ &\quad + \frac{1}{\kappa(\mathbf{p})} \hat{\boldsymbol{\alpha}}^* \hat{\boldsymbol{\alpha}}^T \end{aligned} \quad (39)$$

using (10) and (11). Next, since $\kappa(\mathbf{p})$ is a real number and \mathbf{S}^{-1} is Hermitian, we have $\hat{\boldsymbol{\alpha}}^* = \kappa(\mathbf{p}) \mathbf{Z}^H \mathbf{S}^{-1} \mathbf{p} = \kappa(\mathbf{p}) \mathbf{u}$ from (10) and (38). Thus, the second, third, and last terms in the right-hand side of (39) can be written as

$$\hat{\boldsymbol{\alpha}}^* \mathbf{p}^H \mathbf{S}^{-1} \mathbf{Z} = \kappa(\mathbf{p}) \mathbf{u}\mathbf{u}^H, \quad (40)$$

$$\mathbf{Z}^H \mathbf{S}^{-1} \mathbf{p} \hat{\boldsymbol{\alpha}}^T = \mathbf{u} \hat{\boldsymbol{\alpha}}^T, \quad (41)$$

and

$$\frac{1}{\kappa(\mathbf{p})} \hat{\boldsymbol{\alpha}}^* \hat{\boldsymbol{\alpha}}^T = \mathbf{u} \hat{\boldsymbol{\alpha}}^T, \quad (42)$$

respectively. Using (40)-(42) in (39), we can obtain (37).

Now, since $|\mathbf{A}\mathbf{B}| = |\mathbf{A}||\mathbf{B}|$ for square matrices \mathbf{A} and \mathbf{B} of the same size [31] and $|\mathbf{I}_m + \mathbf{A}\mathbf{B}| = |\mathbf{I}_n + \mathbf{B}\mathbf{A}|$ for any $m \times n$ matrix \mathbf{A} and $n \times m$ matrix \mathbf{B} [33], the numerator in the left-hand side of (12) can be written as

$$\begin{aligned} |\mathbf{R}(\mathbf{0}_{L \times 1}) + \mathbf{S}| &= |\mathbf{S}(\mathbf{I}_N + \mathbf{S}^{-1} \mathbf{Z}\mathbf{Z}^H)| \\ &= |\mathbf{S}| |\mathbf{I}_L + \Upsilon| \\ &= |\mathbf{S}| |\mathbf{X}|. \end{aligned} \quad (43)$$

Following similar steps, the term $|\mathbf{R}(\hat{\boldsymbol{\alpha}}) + \mathbf{S}|$ in the denominator in the left-hand side of (12) can be expressed as

$$\begin{aligned} |\mathbf{R}(\hat{\boldsymbol{\alpha}}) + \mathbf{S}| &= \left| \mathbf{S} + (\mathbf{Z} - \mathbf{p}\hat{\boldsymbol{\alpha}}^T) (\mathbf{Z} - \mathbf{p}\hat{\boldsymbol{\alpha}}^T)^H \right| \\ &= |\mathbf{S}| \left| \mathbf{I}_L + (\mathbf{Z} - \mathbf{p}\hat{\boldsymbol{\alpha}}^T)^H \mathbf{S}^{-1} (\mathbf{Z} - \mathbf{p}\hat{\boldsymbol{\alpha}}^T) \right|. \end{aligned} \quad (44)$$

Now, with the result (37), we can rewrite (44) as

$$\begin{aligned} |\mathbf{R}(\hat{\boldsymbol{\alpha}}) + \mathbf{S}| &= |\mathbf{S}| |\mathbf{X} - \kappa(\mathbf{p}) \mathbf{u}\mathbf{u}^H| \\ &= |\mathbf{S}| |\mathbf{X}| \left| \mathbf{I}_L - \kappa(\mathbf{p}) \mathbf{X}^{-1} \mathbf{u}\mathbf{u}^H \right| \\ &= |\mathbf{S}| |\mathbf{X}| (1 - \kappa(\mathbf{p}) \mathbf{u}^H \mathbf{X}^{-1} \mathbf{u}). \end{aligned} \quad (45)$$

From (43) and (45), we get (13) after a few straightforward steps.

APPENDIX B

PROOF OF THE CFAR PROPERTY OF THE LRT (31)

We will prove the CFAR property of the LRT (31) by showing that the distribution of the maximum eigenvalue d_{\max} of Υ under the null hypothesis does not depend on the noise covariance matrix \mathbf{C} .

Let us first decompose \mathbf{C} as

$$\mathbf{C} = \mathbf{U}_C^H \boldsymbol{\Lambda}_C \mathbf{U}_C, \quad (46)$$

where \mathbf{U}_C is an $N \times N$ unitary matrix such that $\mathbf{U}_C^{-1} = \mathbf{U}_C^H$ and $\boldsymbol{\Lambda}_C$ is the $N \times N$ diagonal matrix composed of the eigenvalues of \mathbf{C} . Next, define

$$\tilde{\mathbf{Z}} = \mathbf{Q}^{-1} \mathbf{Z} \quad (47)$$

and

$$\tilde{\mathbf{Z}}_S = \mathbf{Q}^{-1} \mathbf{Z}_S, \quad (48)$$

where

$$\mathbf{Q} = \mathbf{U}_C^H \boldsymbol{\Lambda}_C^{1/2} \mathbf{U}_C \quad (49)$$

with $\Lambda_C^{1/2}$ denoting the $N \times N$ diagonal matrix of the square roots of the diagonal elements of Λ_C : Note that the diagonal elements of Λ_C are positive since C is positive definite. Then, under the null hypothesis, we have $\tilde{\mathbf{Z}} = [\mathbf{Q}^{-1}\mathbf{n}_1, \mathbf{Q}^{-1}\mathbf{n}_2, \dots, \mathbf{Q}^{-1}\mathbf{n}_L]$ and $\tilde{\mathbf{Z}}_S = [\mathbf{Q}^{-1}\mathbf{n}_{L+1}, \mathbf{Q}^{-1}\mathbf{n}_{L+2}, \dots, \mathbf{Q}^{-1}\mathbf{n}_{L+K}]$: Thus, for any column of $\tilde{\mathbf{Z}}$ and $\tilde{\mathbf{Z}}_S$, we have

$$\begin{aligned} E \left[(\mathbf{Q}^{-1}\mathbf{n}_j) (\mathbf{Q}^{-1}\mathbf{n}_j)^H \right] &= \mathbf{Q}^{-1} E [\mathbf{n}_j \mathbf{n}_j^H] (\mathbf{Q}^{-1})^H \\ &= \mathbf{Q}^{-1} \mathbf{C} (\mathbf{Q}^{-1})^H \\ &= \mathbf{I}_N, \end{aligned} \tag{50}$$

which implies that the distributions of $\tilde{\mathbf{Z}}$ and $\tilde{\mathbf{Z}}_S$ do not depend on C .

Finally, since Υ can be expressed as

$$\begin{aligned} \Upsilon &= \tilde{\mathbf{Z}}^H \mathbf{Q}^H \left(\mathbf{Q} \tilde{\mathbf{Z}}_S \tilde{\mathbf{Z}}_S^H \mathbf{Q}^H \right)^{-1} \mathbf{Q} \tilde{\mathbf{Z}} \\ &= \tilde{\mathbf{Z}}^H \left(\tilde{\mathbf{Z}}_S \tilde{\mathbf{Z}}_S^H \right)^{-1} \tilde{\mathbf{Z}} \end{aligned} \tag{51}$$

from $\mathbf{S} = \mathbf{Z}_S \mathbf{Z}_S^H = \mathbf{Q} \tilde{\mathbf{Z}}_S \tilde{\mathbf{Z}}_S^H \mathbf{Q}^H$, it is clear that, under the null hypothesis, the distribution of the maximum eigenvalue d_{\max} of Υ does not depend on the noise covariance matrix C .

ACKNOWLEDGMENT

This work was supported by the National Research Foundation of Korea under Grant NRF-2015R1A2A1A01005868 with funding from the Ministry of Science, Information and Communications Technology, and Future Planning, for which the authors wish to express their appreciation.

REFERENCES

- [1] S. M. Kay, *Fundamentals of Statistical Signal Processing: Detection Theory*. New Jersey, USA: Prentice Hall, 1998.
- [2] E. Conte and M. Longo, "Characterisation of radar clutter as a spherically invariant random process," *IEE Proc.*, vol. 134, no. 2, pp. 191-197, Apr. 1987.
- [3] N. Bon, A. Khenchaf, and R. Garello, "GLRT subspace detection for range and Doppler distributed targets," *IEEE Trans. Aerosp., Electron. Syst.*, vol. 44, no. 2, pp. 678-696, Apr. 2008.
- [4] K. Gerlach, "Spatially distributed target detection in non-Gaussian clutter," *IEEE Trans. Aerosp., Electron. Syst.*, vol. 35, no. 3, pp. 926-934, July 1999.

- [5] E. Conte, A. D. Maio, and G. Ricci, "GLRT-based adaptive detection algorithms for range-spread targets," *IEEE Trans. Signal Process.*, vol. 49, no. 7, pp. 1336-1348, July 2001.
- [6] K. Gerlach and M. J. Steiner, "Adaptive detection of range distributed targets," *IEEE Trans. Signal Process.*, vol. 47, no. 7, pp. 1844-1851, July 1999.
- [7] K. Gerlach and M. J. Steiner, "Fast converging adaptive detection of Doppler-shifted, range-distributed targets," *IEEE Trans. Signal Process.*, vol. 48, no. 9, pp. 2686-2690, Sep. 2000.
- [8] E. Conte, A. D. Maio, and G. Ricci, "CFAR detection of distributed targets in non-Gaussian disturbance," *IEEE Trans. Aerosp. Electron. Syst.*, vol. 38, no. 2, pp. 612-621, Apr. 2002.
- [9] A. D. Maio, A. Farina, and K. Gerlach, "Adaptive detection of range spread targets with orthogonal rejection," *IEEE Trans. Aerosp., Electron. Syst.*, vol. 43, no. 2, pp. 738-752, Apr. 2007.
- [10] Y. He, T. Jian, F. Su, C. Qu, and X. Gu, "Novel range-spread target detectors in non-Gaussian clutter," *IEEE Trans. Aerosp. Electron. Syst.*, vol. 46, no. 3, pp. 1312-1327, July 2010.
- [11] G. A. Fabrizio, A. Farina, and M. D. Turley, "Spatial adaptive subspace detection in OTH radar," *IEEE Trans. Aerosp. Electron. Syst.*, vol. 39, no. 4, pp. 1407-1428, Oct. 2003.
- [12] S. Ramprashad, T. W. Parks, and R. Shenoy, "Signal modeling and detection using cone classes," *IEEE Trans. Signal Process.*, vol. 4, no. 2, pp. 329-338, Feb. 1996.
- [13] L. L. Scharf and B. Friedlander, "Matched subspace detectors," *IEEE Trans. Signal Process.*, vol. 42, no. 8, pp. 2146-2157, Aug. 1994.
- [14] S. Kraut, L. L. Scharf, and L. T. McWhorter, "Adaptive subspace detectors," *IEEE Trans. Signal Process.*, vol. 49, no. 1, pp. 1-16, Jan. 2001.
- [15] O. Besson and L. L. Scharf, "CFAR matched direction detector," *IEEE Trans. Signal Process.*, vol. 54, no. 7, pp. 2840-2844, July 2006.
- [16] O. Besson, L. L. Scharf, and S. Kraut, "Adaptive detection of a signal known only to lie on a line in a known subspace, when primary and secondary data are partially homogeneous," *IEEE Trans. Signal Process.*, vol. 54, no. 12, pp. 4698-4705, Dec. 2006.
- [17] F. Bandiera, A. D. Maio, A. S. Greco, and G. Ricci, "Adaptive radar detection of distributed targets in homogeneous and partially homogeneous noise plus subspace interference," *IEEE Trans. Signal Process.*, vol. 55, no. 4, pp. 1223-1237, Apr. 2007.
- [18] W. Liu, J. Liu, L. Huang, K. Yan, and Y. Wang, "Adaptive double subspace signal detection in Gaussian background—Part 1: Homogeneous environments," *IEEE Trans. Signal Process.*, vol. 62, no. 9, pp. 2345-2357, May 2014.
- [19] A. Aubry, A. D. Maio, D. Orlando, and M. Piezzo, "Adaptive detection of point-like targets in the presence of homogeneous clutter and subspace interference," *IEEE Signal Process. Lett.*, vol. 21, no. 7, pp. 848-852, July 2014.
- [20] W. Liu, W. Xie, and J. Liu, "Robust GLRT approaches to signal detection in the presence of spatial-temporal uncertainty," *Signal Process.*, vol. 118, pp. 272-284, Jan. 2016.

- [21] A. D. Maio, "Robust adaptive radar detection in the presence of steering vector mismatches," *IEEE Trans. Aerosp. Electron. Syst.*, vol. 41, no. 4, pp. 1322-1337, Oct. 2005.
- [22] F. Bandiera, A. D. Maio, and G. Ricci, "Adaptive CFAR radar detection with conic rejection," *IEEE Trans. Signal Process.*, vol. 55, no. 6, pp. 2533-2541, June 2007.
- [23] A. D. Maio, S. D. Nicola, Y. Huang, S. Zhang, and A. Farina, "Adaptive detection and estimation in the presence of useful signal and interference mismatches," *IEEE Trans. Signal Process.*, vol. 57, no. 2, pp. 436-450, Feb. 2009.
- [24] F. Bandiera, D. Orlando, and G. Ricci, "CFAR detection strategies for distributed targets under conic constraints," *IEEE Trans. Signal Process.*, vol. 57, no. 9, pp. 3305-3316, Sep. 2009.
- [25] A. Svensson and A. Jakobsson, "Adaptive detection of a partly known signal corrupted by strong interference," *IEEE Signal Process. Lett.*, vol. 18, no. 12, pp. 729-732, Dec. 2011.
- [26] E. J. Kelly, "An adaptive detection algorithm," *IEEE Trans. Aerosp., Electron. Syst.*, vol. 22, no. 1, pp. 115-127, Mar. 1986.
- [27] E. J. Kelly and K. Forsythe, "Adaptive detection and parameter estimation for multidimensional signal models," Lincoln Lab., Mass. Inst., Technol., Lexington, USA, Tech. Rep. no. 848, Apr. 1989.
- [28] T. Roh and L. Vandenberghe, "Discrete transforms, semidefinite programming and sum-of-squares representations of nonnegative polynomials," *SIAM J. Optim.*, vol. 16, no. 4, pp. 939-964, Jan. 2006.
- [29] L. Vandenberghe and S. Boyd, "Semidefinite programming," *SIAM Review*, vol. 38, no. 1, pp. 49-95, Mar. 1996.
- [30] A. D. Maio, S. D. Nicola, A. Farina, and S. Iommelli, "Adaptive detection of a signal with angle uncertainty," *IET Radar, Sonar, Navigation*, vol. 4, no. 4, pp. 537-547, Aug. 2010.
- [31] S. H. Friedberg, A. J. Insel, and L. E. Spence, *Linear Algebra*. New Jersey, USA: Prentice-Hall, 1979.
- [32] Y. Saad, *Numerical Methods for Large Eigenvalue Problems: Revised Edition*. Philadelphia, USA: SIAM, 2011.
- [33] R. Horn and C. Johnson, *Matrix Analysis*. Cambridge, U.K.: Cambridge Univ. Press, 1985.
- [34] S. Lang, *Linear Algebra*. New York, USA: Springer-Verlag, 1987.
- [35] P. K. Hughes II, "A high resolution radar detection strategy," *IEEE Trans. Aerosp., Electron. Syst.*, vol. 19, no. 5, pp. 663-667, Sep. 1983.
- [36] M. Skolnik, *Radar Handbook*. Third ed. New York, NJ, USA: McGraw-Hill, 2008.